

Dopant induced stabilization of Silicon cluster at finite temperature.

Shahab Zorriastain, Kavita Joshi, and D. G. Kanhere
*Department of Physics, and Center for Modeling and Simulation,
 University of Pune, Ganeshkhind, Pune-411 007, India*
 (Dated: February 6, 2008)

With the advances in miniaturization, understanding and controlling properties of significant technological systems like silicon in nano regime assumes considerable importance. The small silicon clusters in the size range of 15-20 atoms are known to fragment upon heating. In the present work we demonstrate that it is possible to stabilize such clusters by introducing appropriate dopant (in this case Ti). Specifically, by using the first principle density functional simulations we show that Ti doped Si_{16} , having the Frank-Kasper geometry, remains stable till 2200 K and fragments only above 2600 K. The observed melting transition is a two step process. The first step is initiated by the surface melting around 600 K. The second step is the destruction of the cage which occurs around 2250 K giving rise to a peak in the heat capacity curve.

PACS numbers: 31.15.Ew, 31.15.Qg, 36.40.Ei, 36.40.Qv

I. INTRODUCTION

With the advent of nano science and technology, investigating physical properties of clusters has assumed considerable importance.¹ As the size of the system becomes smaller and smaller its physical and chemical properties are expected to change, sometimes significantly. In fact, this is what drives the quest for nano materials research. However, it may happen that this size effect could drive a property towards an undesirable direction. The finite temperature properties of small silicon clusters is one such example. In our recent finite temperature studies² it was found that the small clusters of silicon (Si_n , $n=15$ and 20) become unstable and fragment when heated up to about 1500 K. Typically, our extensive density functional simulations showed that Si_{15} fragments around 1800 K in to Si_9 and Si_6 , although we also observe $\text{Si}_{10}+\text{Si}_5$ and Si_8+Si_7 for a short time span. It exists in a liquid like phase over a short temperature range (900 to 1400 K) before fragmenting. On the other hand, Si_{20} transforms from the ground state to the first isomer (with two distinct Si_{10} units) around 1000 K and eventually fragments in to two Si_{10} units around 1200 K. Thus, Si_{20} does not show any solid-like to liquid-like transition prior to fragmentation. The result although not surprising, can have technological implications, silicon being the key ingredient in most of the semiconductor devices. The present work addresses the issue of remedying this difficulty by using appropriate dopant. That the impurities induce significant changes in the structure as well as electronic properties is well known in the solid state community. In the context of clusters several studies have been reported. For example, single atom of tin or aluminum in lithium clusters are known to change the nature of bonding among the host atoms.^{3,4} In a recent work Mottet *et. al.*⁵ demonstrated that a single impurity (Ni or Cu) in Ag_{55} cluster changes structural and thermal properties dramatically. Interestingly, this effect was found to be significant only on an icosahedral host.

Silicon is the most important semiconducting materials in the microelectronics industry. In medium-sized regime, the structure and properties of materials often differ dramatically from those of the bulk. Over the past several years there have been extensive theoretical and experimental work describing the ground state geometries of medium sized silicon clusters.^{6,7,8,9,10,11} These clusters are built upon stable tricapped trigonal prism (TTP) units which plays a crucial role in the finite temperature behavior of the cluster.¹¹ The high stability of TTP units results in to fragmentation of these clusters instead of solid-like to liquid-like transition.² The ground state geometries of these clusters are well established in the literature. The ground state geometry of Si_{16} can be described as two fused pentagonal prisms.⁸

Experiments on doped silicon clusters Si_nM ($\text{M}=\text{Ti}, \text{Hf}, \text{Cr}, \text{Mo}$, and W) have shown large abundances for $n = 15, 16$ and low intensities for other sizes.^{12,13,14} Specifically the abundances drop drastically beyond $n = 16$, giving support to the predictions of the exceptional stability of $n = 16$ clusters. Vijay Kumar and co-workers¹⁶ showed that for $n = 8 - 12$ basket-like open structures to be the most favorable, while for $n = 13 - 16$, the metal atom is completely surrounded by silicon atoms. Recently, measurements of electron affinities of Ti-doped silicon clusters¹² have been found to have a minimum at $n = 16$, suggesting the closed electronic shell nature and strong stability of Si_{16}Ti . The electronic structure of silicon clusters in the size range noted above has been studied by *ab initio* methods.^{6,7,8} It may be noted that none of the silicon clusters in this size range form stable caged structures. In a quest to obtain stable silicon cage structures, Vijay Kumar and co-workers^{15,16,17,18} found that it is possible to stabilize a caged structure for cluster using a class of dopants. Specifically, they showed that a single impurity of transition metal atoms like Ti, Zr, Hf enhances the binding energy of Si_{16} and changes the structure to a caged one, similar to carbon cages. The gain in binding energy is substantial and is of the

order of few eV and HOMO-LUMO gap is more than 1 eV which make these structures stable. Among the systems studied, Si_{16}Ti has the largest HOMO-LUMO gap (2.35 eV) as compared to other dopants of Si_{16} like Zr and Hf.¹⁵ The ground state geometry for Si_{16}Ti has been found to be a Frank Kasper polyhedron, which is also shown in Fig. 1-a. Therefore Si_{16}Ti is a likely candidate to show a stable behavior at finite temperatures. As we shall demonstrate, by adding a dopant like Ti, we could avoid the fragmentation observed in small Si clusters. The cluster shows a surface melting of Si atoms. However, the motion of Si atoms is restricted to a small shell around Ti until 2200 K. The cluster is on the verge of fragmentation around 2600 K, almost 1000 K higher than that in pure Si clusters.

II. COMPUTATIONAL DETAILS

We have carried out isokinetic Born–Oppenheimer Molecular Dynamic (BOMD) simulations using ultra-soft pseudopotentials within the Generalized Gradient Approximation (GGA), as implemented in the VASP package.¹⁹ For computing heat capacities, the BOMD calculations were carried out for 17 different temperatures in the range of 100 K to 3000 K, each with the duration of 150 ps or more, which result in to a total simulation time of 2.6 ns. In order to get converged heat capacity curve especially in the region of coexistence, more temperatures were required with longer simulation times. We have discarded the first 30 ps of each temperature for thermalization. To analyze the thermodynamic properties, we first calculate the ionic specific heat by using the Multiple Histogram (MH) technique.^{20,21} We extract the classical ionic density of states ($\Omega(E)$) of the system, or equivalently the classical ionic entropy, $S(E) = k_B \ln \Omega(E)$ following the MH technique. With $S(E)$ in hand, one can evaluate thermodynamic averages in a variety of ensembles. We focus in this work on the ionic specific heat and the caloric curve. In the canonical ensemble, the specific heat is defined as usual by $C(T) = \partial U(T)/\partial T$, where $U(T) = \int E p(E, T) dE$ is the average total energy, and where the probability of observing an energy E at a temperature T is given by the Gibbs distribution $p(E, T) = \Omega(E) \exp(-E/k_B T)/Z(T)$, with $Z(T)$ the normalizing canonical partition function. We normalize the calculated canonical specific heat by the zero-temperature classical limit of the rotational plus vibrational specific heat, i.e., $C_0 = (3N - 9/2)k_B$.

We have calculated the root-mean-square bond length fluctuations (δ_{rms}) for Si-Si and Si-Ti bonds separately to compare the difference between them. The δ_{rms} is defined as

$$\delta_{\text{rms}} = \frac{1}{N} \sum_{i>j} \frac{(\langle r_{ij}^2 \rangle_t - \langle r_{ij} \rangle_t^2)^{1/2}}{\langle r_{ij} \rangle_t}, \quad (1)$$

where N is the number of bonds in the system ($N=120$ for Si-Si, and $N=16$ for Si-Ti), r_{ij} is the distance between

atoms i and j , and $\langle \dots \rangle_t$ denotes a time average over the entire trajectory. Mean Square Displacement (MSD) is another traditional parameter used for determining phase transition and is defined as,

$$\langle \mathbf{r}^2(t) \rangle = \frac{1}{NM} \sum_{m=1}^M \sum_{I=1}^N [\mathbf{R}_I(t_{0m} + t) - \mathbf{R}_I(t_{0m})]^2 \quad (2)$$

here N is the number of atoms in the system ($N=16$ for Si and $N=1$ for Ti) and R is the position of the I^{th} atom. Here we average over M different time origins t_{0m} spanning over the entire trajectory. The interval between the consecutive t_{0m} for the average was taken to be about 0.3 ps. The MSD of a cluster indicate the displacement of atoms in the cluster as a function of time.

We have also calculated radial distribution function ($g(r)$) and deformation parameter (ε_{def}). $g(r)$ is defined as the average number of atoms within the region r and $r+dr$. The shape deformation parameter (ε_{def}) is defined as,

$$\varepsilon_{\text{def}} = \frac{2Q_x}{Q_y + Q_z}, \quad (3)$$

where $Q_x \geq Q_y \geq Q_z$ are the eigenvalues, in descending order, of the quadrupole tensor

$$Q_{ij} = \sum_I R_{Ii} R_{Ij}. \quad (4)$$

Here i and j run from 1 to 3, I runs over the number of ions, and R_{Ii} is the i^{th} coordinate of ion I relative to the COM of the cluster. A spherical system ($Q_x = Q_y = Q_z$) has $\varepsilon_{\text{def}}=1$ and larger values of ε_{def} indicates deviation of the shape of the cluster from sphericity. We use the electron localization function (ELF)²² to investigate the nature of bonding. For a single determinantal wave function built from Kohn-Sham orbitals ψ_i , the ELF is defined as

$$\chi_{\text{ELF}} = [1 + (D/D_h)^2]^{-1}, \quad (5)$$

where

$$D_h = (3/10)(3\pi^2)^{5/3} \rho^{5/3}, \quad (6)$$

$$D = (1/2) \sum_i |\nabla \psi_i|^2 - (1/8) |\nabla \rho|^2 / \rho, \quad (7)$$

with $\rho \equiv \rho(\mathbf{r})$ is the valence-electron density. The ELF is defined in such a way that its value is unity for completely localized systems and 0.5 for homogeneous electron gas.

III. RESULTS AND DISCUSSION

We begin our discussion by noting the ground state (GS) and some low lying structures of Si_{16}Ti which are shown in Fig. 1. As has been already mentioned the ground state of Si_{16}Ti is Frank-Kasper polyhedron. The

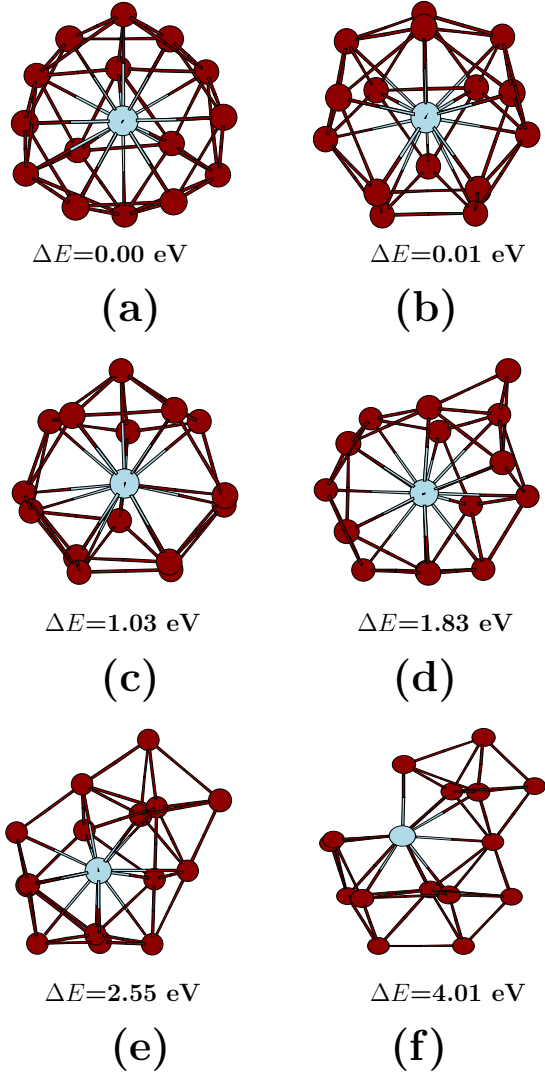


FIG. 1: The ground state geometry and few interesting isomers of Si_{16}Ti

central Ti atom is surrounded by 16 Si atoms within two closely spaced shells one with 12 atoms, all equidistant from central Ti atom and another shell consisting of 4 Si atoms forming a tetrahedron with Ti at the center. The first isomer (Fig. 1-b) is energetically very close to the ground state where all Si atoms are nearly equidistant from central Ti atom ($\Delta E = .009 \text{ eV}$). Isomers with either distorted cage of Si atoms or without Si cage are quite high in energy compared to the lowest two structures. Isomer shown in Fig. 1-f occurs at very high temperature (around 2600 K) and indicates possible path for fragmentation. At this point its interesting to compare pure silicon clusters with doped clusters. Si clusters have very interesting growth pattern. The ground state geometries of Si_n till $n = 22$ are prolate and for larger sizes the GS transforms into spherical structures. It has been also observed that a TTP unit is a part of prolate ground states. Presence of highly stable TTP unit also bypass

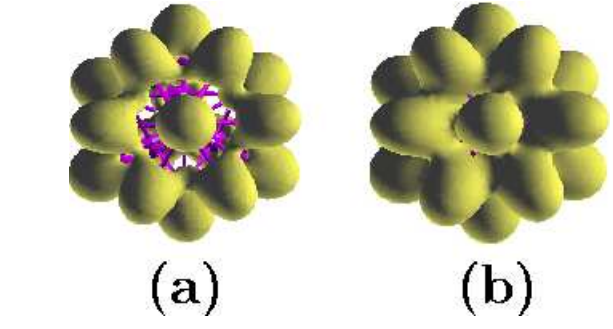


FIG. 2: The isosurfaces of ELF at $\chi_{\text{ELF}}=0.70$ and $\chi_{\text{ELF}}=0.55$ are shown in (a) and (b) respectively.

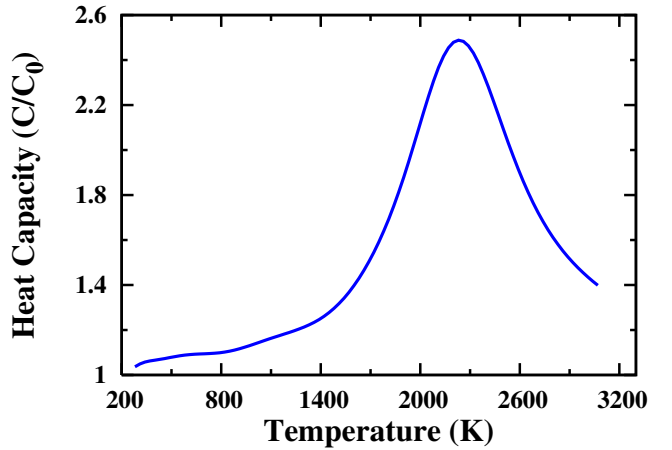


FIG. 3: The heat capacity for Si_{16}Ti computed over last 120 ps. The peak is at 2250 K.

the liquid-like state and leads to fragmentation of pure Si_n clusters around 1200 K to 1800 K in the size range of 15-20. Further, the ground state of Si_{16} is a prolate structure and a cage like isomer is found to be difficult to stabilize.

The nature of bonding in Si_{16}Ti can be discussed by examining the iso-surfaces of total charge density and ELF. In Fig. 2 we show the iso-surface of ELF for value of 0.7 (Fig. 2-a) and 0.55 (Fig. 2-b). At higher values of χ_{ELF} the figure clearly shows localization of the charge on hexagonal rings depicting the covalent nature of bonding. These atoms are connected to each other by the shortest bonds (2.37-2.43 Å) and are connected to the remaining four Si atoms at very low value of $\chi_{\text{ELF}} \approx 0.60$ (bondlengths around 2.65 Å). The bonding between silicon atoms belonging to two different shells is metallic like in the sense it is due to delocalized charge distribution.

Next we show the ionic heat capacity of Si_{16}Ti in Fig. 3. The heat capacity displays a broad melting peak at 2250 K characteristic of a finite size system. A more careful observation of ionic motions and traditional parameters like δ_{rms} reveals that the main peak in the heat capacity is related to complete breakdown of Si cage and

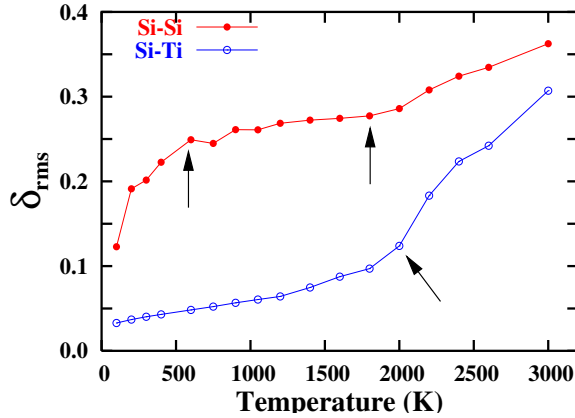


FIG. 4: The δ_{rms} for Si-Si bonds (online red color) and Si-Ti bonds (online blue color) are shown. The region between 600 K to 1800 K (shown by arrows for Si-Si bonds) corresponds to ‘restricted’ liquid-like behavior of Si cage. The rise in δ_{rms} observed after 2000 K (shown by arrow for Si-Ti bonds) is associated with the breaking of Si cage and diffusion of Ti through out the cluster.

escape of Ti atom from the cage. The δ_{rms} for Si-Si and Si-Ti bonds, shown in Fig. 4, throws light on the finite temperature behavior of this cluster. The value of δ_{rms} for Si-Si bonds is considerably high at much lower temperatures (around 200 K) whereas the value of δ_{rms} for Si-Ti bonds is quite low till 1800 K. The higher value of δ_{rms} for Si atoms indicates that Si atoms are mobile at low temperatures. More detailed analysis of ionic motion reveals that the cluster undergoes isomerization around as low temperature as 100 K. The cluster transforms from the GS to the first isomer and back to the GS which in turn results in to diffusion of at least 4 atoms. The MSD also support this observation. In Fig. 5 and Fig. 6 the MSD computed for Si and Ti atoms at some relevant temperatures are shown respectively. As can be noted from Fig. 5 the MSD for Si atoms saturate around 600 K indicating that the atoms are diffusing on the spherical shell around Ti atom and the cluster is partially melted. On the contrary, as can be seen from Fig. 6 the Ti atom shows very small displacement till 2000 K. Although the MSD shows liquid-like behavior around much lower temperature (600 K) the Si atoms are confined to a small shell around Ti (preserving the spherical shape) until quite high temperatures. Its only around 2000 K or so that the Si cage breaks down giving rise to a peak in the heat capacity around 2200 K. That the motion of Si atoms is restricted to a shell is clear from the examination of radial distribution function.

In Fig. 7 we show the radial distribution function calculated from the center of mass (Ti site) for some representative temperatures. The peak near origin is due to the Ti atom whereas a single peak around 2.8 Å is due to Si cage. The width of this peak does not change significantly till 1600 K. A continuous distribution emerges after 2200 K indicating that the Si cage is destroyed and

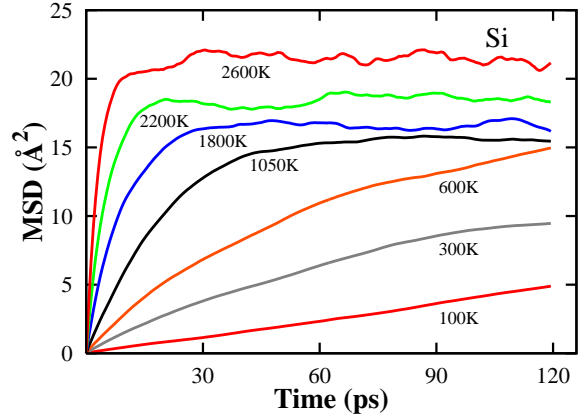


FIG. 5: The MSD calculated for Si atoms for few relevant temperatures.

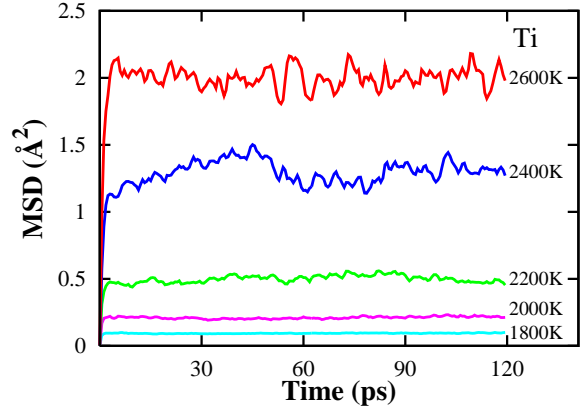


FIG. 6: The MSD calculated for Ti atom for five different temperature

Ti has escaped from the cage. This change is accompanied by the shape change of the cluster.

In Fig. 8 we show shape deformation parameter as a function of temperature. It can be seen that till 2000 K value of ε_{def} is nearly 1 indicating a spherical shape with restricted motion of Si atoms on the surface. The ε_{def} increases significantly above 2000 K indicating the breakdown of Si cage. Our simulation shows that a fragmentation channel opens up around 2600 K possibly because of emergence of central Ti atom on the surface. We have observed that Si_{16}Ti around this temperature fragments into two parts, the most probable fragments are $\text{Si}_{12}\text{Ti} + \text{Si}_4$ and $\text{Si}_{13}\text{Ti} + \text{Si}_3$. A typical configuration leading to fragmentation of Si_{16}Ti is also shown in the Fig. 8.

IV. SUMMARY AND CONCLUSION

To summarize, our DFT simulations clearly demonstrate that its possible to avoid fragmentation of small Si clusters by doping them with appropriate impurity, in

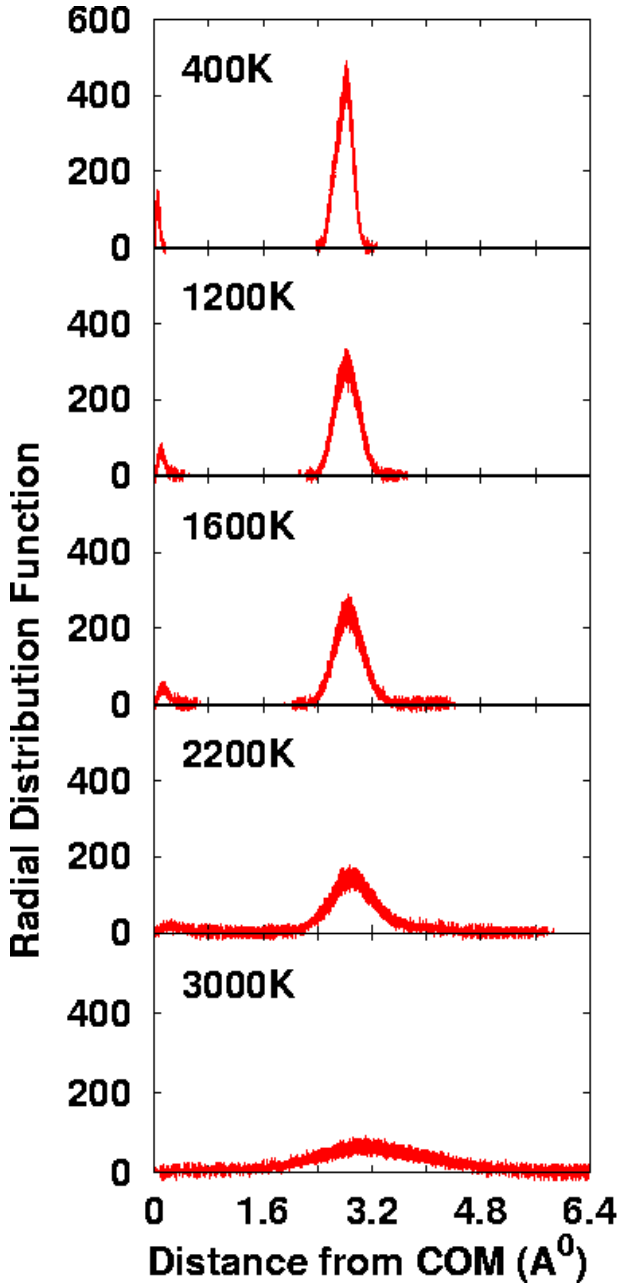


FIG. 7: The radial distribution function calculated for five different temperatures.

this case Ti. Contrary to the pure Si clusters, the doped cluster undergoes a solid-like to liquid-like transition, and remain stable at least up to 2600 K. However, the ‘melting’ occur in two steps, the first one is a low temperature process (around 600 K), where Si atoms diffuse on the shell, whereas the peak in the heat capacity (2250 K) is associated with the breaking of Si cage and escape of Ti atom from the cage. The beginning of the fragmentation is observed around 2600 K which is almost 1000 K higher than that observed in pure Si clusters in this size range.

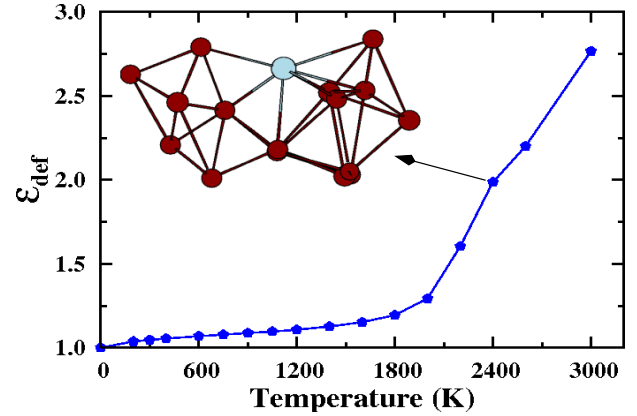


FIG. 8: The deformation parameter is plotted as a function of temperature. Note the sudden rise in the deformation parameter after 2000 K. A typical configuration shown in the Fig occurs around 2400 K, and indicates possible path for fragmentation.

V. ACKNOWLEDGMENT

KJ and DGK thank Indo French Center for Promotion of Advanced Research (IFCPAR) for partial financial support(project No; 3104-2). The authors also thanks M-S Lee for many useful discussions.

¹ P. G. Reinhard, E . Suraud, *Introduction to Cluster Dynamics* (Wiley-VCH, 2004).

² S. Krishnamurty, K. Joshi, D. G. Kanhere, and S. A. Blundell, Phys. Rev. B. **73**, 045419 (2006).

³ K. Joshi and D. G. Kanhere, J. Chem. Phys. **119**, 12301 (2003). M.-S. Lee, D. G. Kanhere, and K. Joshi, Phys. Rev. A. **72**, 015201 (2005).

⁴ H.-P. Cheng, R. N. Barnett, and U. Landman, Phys. Rev. B. **48**, 1820 (1993).

⁵ C. Mottet, G. Rossi, F. Baletto, and R. Ferrando, Phys.

Rev. Lett. **95**, 035501 (2005).

⁶ K.-M. Ho, A.A. Shvartsburg, B. Pan, Z.Y. Lu, C.Z Wang, J.G. Wacker, J.L. Fye, and M.F. Jarrold, Nature, **392**, 582 (1998)

⁷ I. Rata, A. A. Shvartsburg, M. Horoi, T.Frauenheim, Siu K. W. Michael, and K. A. Jackson Phys. Rev. Lett. **85**, 546 (2000).

⁸ X. L. Zhu, X. C. Zeng, Y. A. Lei, and B. Pan J. Chem. Phys. **120**, 8985 (2004).

⁹ K.A. Jackson, M. Horoi, I. Chaudhuri, T. Frauenheim, and

- ¹⁰ A. A. Shvartsburg Phys. Rev. Lett. **93**, 013401, (2003).
¹⁰ L. Mitas, J.C. Grossman, I. Stich, and J. Tobik Phys. Rev. Lett. **84**, 1479 (2000)
- ¹¹ J. Muller, B. Liu, A.A. Shvartsburg, S. Ogut, J. R. Cheilikowsky, Siu K. W. Michael, K. M. Ho, and G. Gantefor Phys. Rev. Lett. **85**, 1666 (2000)
- ¹² M. Ohara, K. Koyasu, A. Nakajima, and K. Kaya, Chem. Phys. Lett **371**, 490 (2003).
- ¹³ P. Sen and L. Mitas, Phys. Rev.B **68**, 155404 (2003).
- ¹⁴ V. Kumar, T. M. Briere, and Y. Kawazoe, Phys. Rev.B **68**, 155412 (2003).
- ¹⁵ V. Kumar and Y. Kawazoe, Phys. Rev. Lett. **87**, 045503 (2001).
- ¹⁶ H. Kawamura, V. Kumar, and Y. Kawazoe, Phys. Rev.B **71**, 075423 (2005).
- ¹⁷ V. Kumar and Y. Kawazoe, Phys. Rev.B **65**, 073404 (2002).
- ¹⁸ V. Kumar, A. K.Singh, and Y. Kawazone, Nano Lett. **4**, 677 (2004).
- ¹⁹ Vienna *ab initio* simulation package, Technische Universität Wien (1999); G. Kresse and J. Furthmüller, Phys. Rev. B **54**, 11169 (1996).
- ²⁰ A. M. Ferrenberg, R. H. Swendsen, Phys. Rev. Lett. **61**, 2635 (1988).
- ²¹ P. Labastie and R. L. Whetten *Phys. Rev. Lett.* **65**, 1567 (1990).
- ²² A. D. Becke and K. E. Edgecombe, J. Chem. Phys. **92**, 5397 (1990).